IOSR Journal of Applied Geology and Geophysics (IOSR-JAGG)
e-ISSN: 2321–0990, p-ISSN: 2321–0982.Volume 8, Issue 1 Ser. II (Jan – Feb 2020), PP 45-51
www.iosrjournals.org

Sensitivity analysis of Extended Elastic Impedance (EEI) attributes from Modified Zoeppritz Equation

Balogun A.O[1] and Dagogo, T[1]
[1](*Department of Physics, University of Port Harcourt, Nigeria*)

Abstract: *Lithology and fluid discrimination are the two foremost objectives in any seismic reservoir characterization project. To delineate and predict hydrocarbon reservoirs, based on an understanding of seismic responses resulting from enhanced seismic interpretation and subsurface modeling, a modified form of the Zoeppritz equation was used to generate Extended Elastic Impedance (EEI) logs and volumes. Sensitivity analyses of the absolute Acoustic Impedance and the derived Extended Elastic Impedance (EEI) at zero angle were performed and the results from both of log correlation and crossplot analyses show that at zero incidence angle these attributes exhibit similar response in characterization of the reservoir but the volume analyses show that the sensitivity of the derived equation is more than that of the regular absolute acoustic impedance. The results from the inversion show that Extended Elastic Impedance at zero degree angle of incidence delineates and highlights gas-saturated reservoirs better than the Acoustic Impedance especially in environments where Acoustic Impedance alone cannot delineate hydrocarbon zones.*

Date of Submission: 14-01-2020 Date of acceptance: 01-02-2020

I. Introduction

The product of the P-wave velocity and rock density is the Acoustic Impedance (AI). AI is not an interface property but a rock property [1]. Though the generation of 3-D petrophysical property models and 3-D facies models are based on the AI models [1-2], still AI is a bad fluid indicator where the upper and lower reservoir formations have approximately equal acoustic properties [3]. This limitation and others were resolved by use of the Extended Elastic Impedance (EEI) [4-7]. This work highlights the sensitivity of the Extended Elastic Impedance (EEI) attributes generated from a modified Zoeppritz equation with respect to acoustic impedance in the determination and delineation of hydrocarbon reservoirs.

The Extended Elastic Impedance (EEI) is the modified extension of the Elastic Impedance (EI) method conducted by [7] by replacing the function $sin^2\theta$ due to limitation in angle of incident range, to a new function (tan χ) with a wider range (from –∞ to + ∞) [3-10]. This equation is then multiplied by cos χ for normalization so that reflectivity value is never more than one [3-10]. Elastic impedance (Equation 1) is a generalization of acoustic impedance for non-normal angles of incidence and is a pseudo-property or seismic attribute developed by [4-5].

$$\mathrm{EI}(\theta) = \mathrm{V_P}^{(1+\tan^2\theta)}\mathrm{V_S}^{(-8\mathrm{K}\sin^2\theta)}\rho^{(1-4\mathrm{K}\sin^2\theta)} \qquad 1$$

Though Elastic Impedance provided good results and useful guides for enhanced reservoir characterization, there was restriction of incidence angle [4-5] and another key problem was that EI has strange unit and dimensions therefore their values do not scale correctly for different angles [6-10].

The difference between the Extended Elastic Impedance (EEI) and normalized version of Elastic Impedance (EI) is the change of variable. EEI is a function of χ (an angle in an abstract construction) and EI is a function of θ (an angel in a physical experiment) [6-10]. EEI allows the use of a range of physically non-meaningful incident angles by substituting tanχ for $sin^2\theta$ in the two-term reflectivity equation. Thus, the primary variable now becomes χ rather than θ and it is varied from -90 to 90° [6-10]. The expression for the normalized version of Elastic Impedance (EI) and the Extended Elastic Impedance (EEI) are shown in Equations 2 and 3.

$$\mathrm{EI}(\theta) = \mathrm{V_{P_0}}\rho_0\left[\mathrm{V_P}^{(1+\tan^2\theta)}\mathrm{V_S}^{(-8\mathrm{K}\sin^2\theta)}\rho^{(1-4\mathrm{K}\sin^2\theta)}\right] \qquad 2$$

$$EEI(\chi) = \alpha_0\rho_0 \left[\frac{\alpha}{\alpha_0}\right]^p \left[\frac{\beta}{\beta_0}\right]^q \left[\frac{\rho}{\rho_0}\right]^r \quad 3$$

Where $\alpha = V_P = P - \text{wave velocity}$, $\beta = V_S = S - \text{wave velocity}$,

ρ = density, $p = cos(\chi) - sin(\chi)$, $q = -8Ksin(\chi)$ and $r = cos(\chi) - 4Ksin(\chi)$ 4

α_0, β_0, and ρ_0 : the average of P velocity, S velocity, and density respectively.

K is the average of $\left(\frac{\beta}{\alpha}\right)^2$ in the time/depth interval according to [11].

II. Material And Methods

The materials used for this study are 3D Pre-stack time migrated seismic data and a complete suite of well logs. Basically, we assume a relationship, possibly linear, between the rock physical properties (P- and S-wave velocities, density, impedances, bulk modulus, shear modulus, Lamé's parameter , pseudo-poisson ratio e.t.c) and seismic reflections, that is, the rock attributes of the formations were examined to create a relationship between the petrophysical data and elastic properties. The Extended Elastic Impedance (EEI) log spectrum is generated and inverted to create an EEI (χ) volume output.

Aki-Richards approximation [12] of Zoeppritz equation [13] was reformulated (Equation 5) in terms of Pseudo Poisson' ratio reflectivity, $\Delta q/\text{q}$, rigidity reflectivity, $\Delta\mu/\mu$, and density reflectivity, $\Delta\rho/\rho$ [14 -15], and using the same derivation procedure as in [5] and [7] on the modified Zoeppritz equation, we derived the new Elastic Impedance and Extended Elastic Impedance respectively in terms of Pseudo-Poisson's ratio, rigidity and density (Equations 6 – 7) for effective fluid and lithology discrimination [14 – 15].

$$\frac{1}{2}\frac{\Delta \mathbf{q}}{\mathbf{q}}(\mathbf{1}+\tan^2\theta) + \frac{1}{2}\frac{\Delta\mu}{\mu}\left(\frac{\sec^2\theta}{2} - 4\left(\frac{V_S}{V_P}\right)^2 \sin^2\theta\right) + \frac{1}{2}\frac{\Delta\rho}{\rho}\left(\mathbf{1} - \frac{1}{2}\sec^2\theta\right) \quad 5$$

$$\mathrm{EI}(\theta) = \mathrm{q}^{1+\tan^2\theta}\mu^{\frac{\sec^2\theta}{2} - 4\left(\frac{V_S}{V_P}\right)^2 \sin^2\theta}\rho^{1-\frac{1}{2}\sec^2\theta} \quad 6$$

where P-wave velocity (V_P or α), S-wave velocity (V_S or β), density (ρ), shear modulus (μ) and (q) is Pseudo-Poisson's ratio [14 – 15].

$$EEI(\chi) = \left[36\mathrm{q}_0^2\mu_0\rho_0\right]^{0.5} \left[\frac{\mathrm{q}}{\mathrm{q}_0}\right]^r \left[\frac{\mu}{\mu_0}\right]^s \left[\frac{\rho}{\rho_0}\right]^t \quad 7$$

B_0, q_0, μ_0, and ρ_0 are references values of P-impedance, Pseudo-Poisson ratio, shear modulus and density, respectively [14 – 15].

III. Result and Discussion

Four wells with several zones of interest were analyzed. Gamma log was used to determine the lithology of each zone in the wells. A low gamma value shows a sand formation while shale formations were indicated by high gamma values. Validation of the Extended Elastic Impedance (EEI) attributes from Modified Zoeppritz Equation was carried out by log correlation and crossplot analysis.

Figure 1 shows the correlation between modeled AI, EI (0), derived EI (0) and EEI (0) log for Well 15 and Well 16. The red curves are the derived EEI (0) curves generated at $\chi = 0^\circ$, the blue curves are the Model EI(0) from well-log data, the magenta curves are the derived EI (0) and the yellow curves are the AI generated from well log data. The derived EEI log and EI (0) log and Model EI (0) log at zero degree corresponds to AI as seen by the overlap of the log plots. This indicates that our equations are valid as they approximate the absolute acoustic impedance at zero incidence angle as expected.

Crossplot analysis was carried out in Well 15 and Well 16 for all the target zones to characterize reservoir in terms of fluid type and lithology. Figures 2 - 5 (a – d), show the crossplot of Acoustic Impedance (AI), Elastic Impedance (EI) at zero degree incidence angle, the derived Elastic Impedance (EI) at zero incidence angle and the Extended Elastic Impedance (EEI) at zero degree incidence angle versus Density respectively, for all the target zones. This is a three-dimensional crossplot color coded with Gamma ray. The crossplots show that at zero angle of incidence these attributes exhibit similar response in characterization of the reservoir.

Results of RMS Amplitude Slices

RMS amplitude extraction was performed for the interpreted horizons, within a time window of 25ms in the reservoir. The RMS amplitude attribute relates to the variations in P-impedance over the selected interval.

Figure 6 (a – c) show the extracted RMS amplitude maps for horizons 1b2, 2a and 3b respectively. High RMS amplitude values were observed indicating hydrocarbon zones and low RMS amplitude values observed indicating shale/brine flooded zones. High RMS amplitude values were also observed away from the Wells location indicating possible bypassed hydrocarbon charge areas.

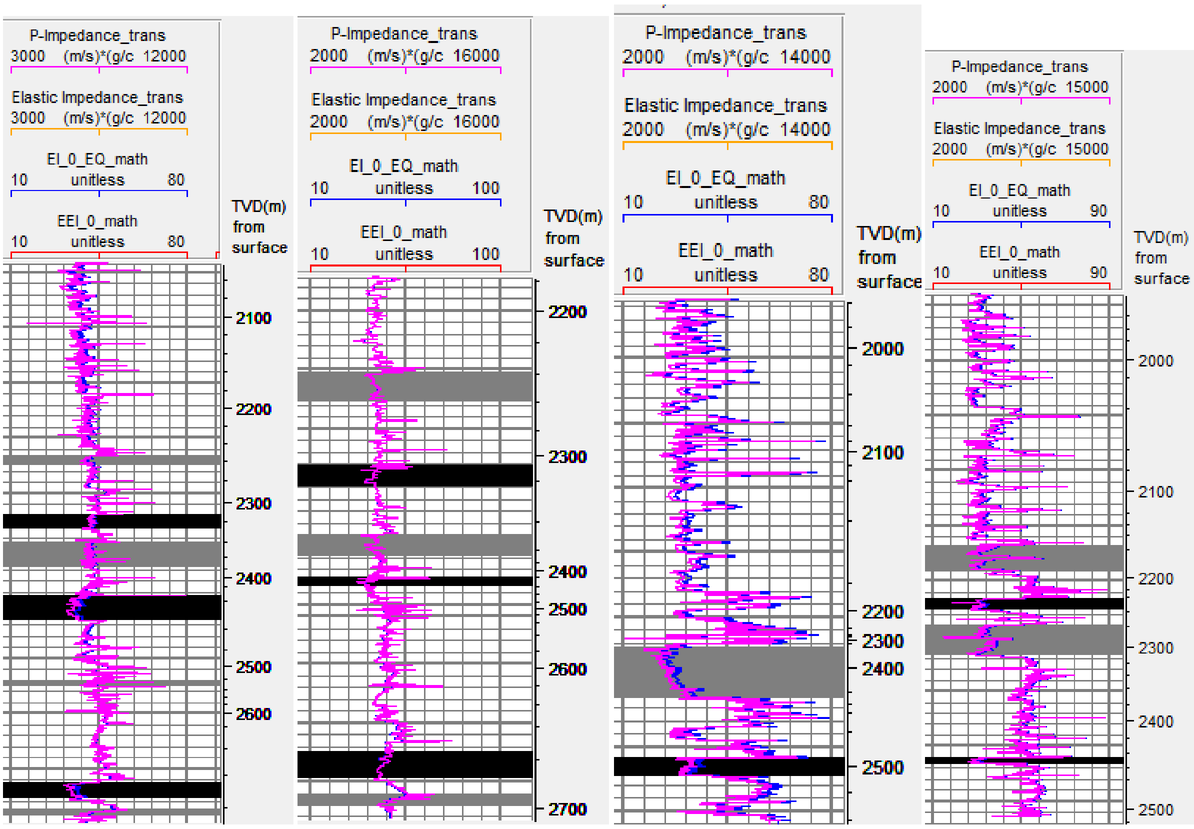

Figure 1: Correlation plots between AI, EI(0) and derived EI (0) and EEI(0)log for Wells 15, 16, 17 and 19

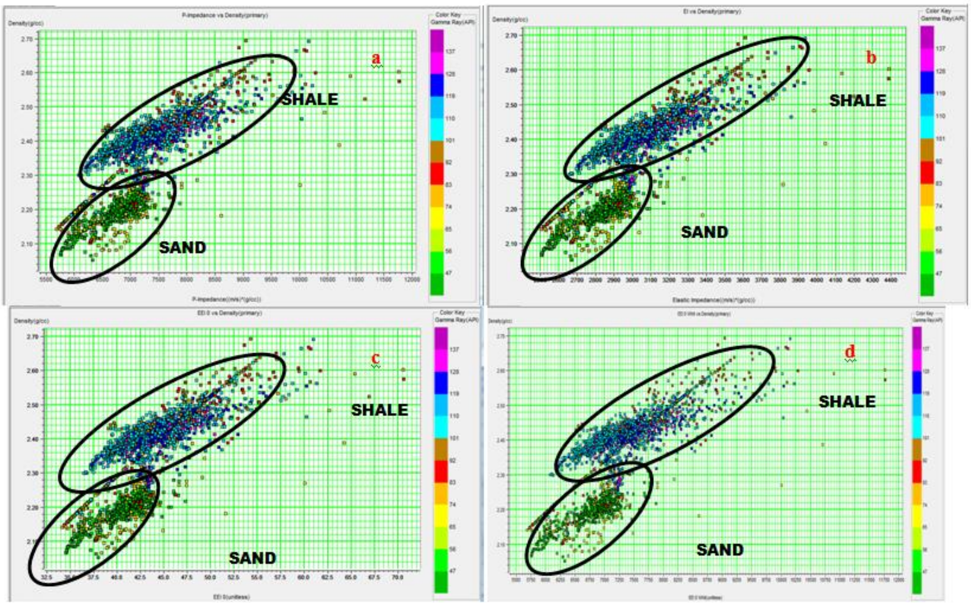

Figure 2: AI, EI(0), Derived EI (0) and Derived EEI(0) versus Density cross plot for all the target zones in Well 15 colour coded with Gamma ray.

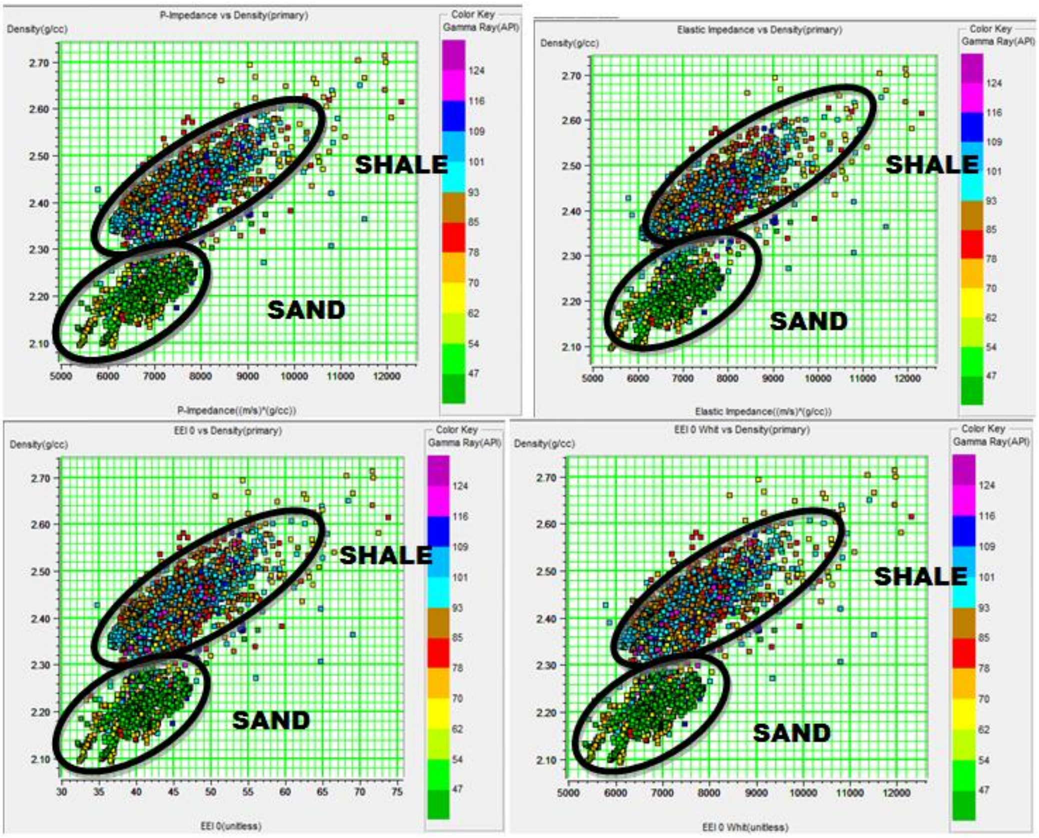

Figure 3: AI, EI (0), Derived EI (0) and Derived EEI(0) versus Density cross plot for all the target zones in Well 16 colour coded with Gamma ray.

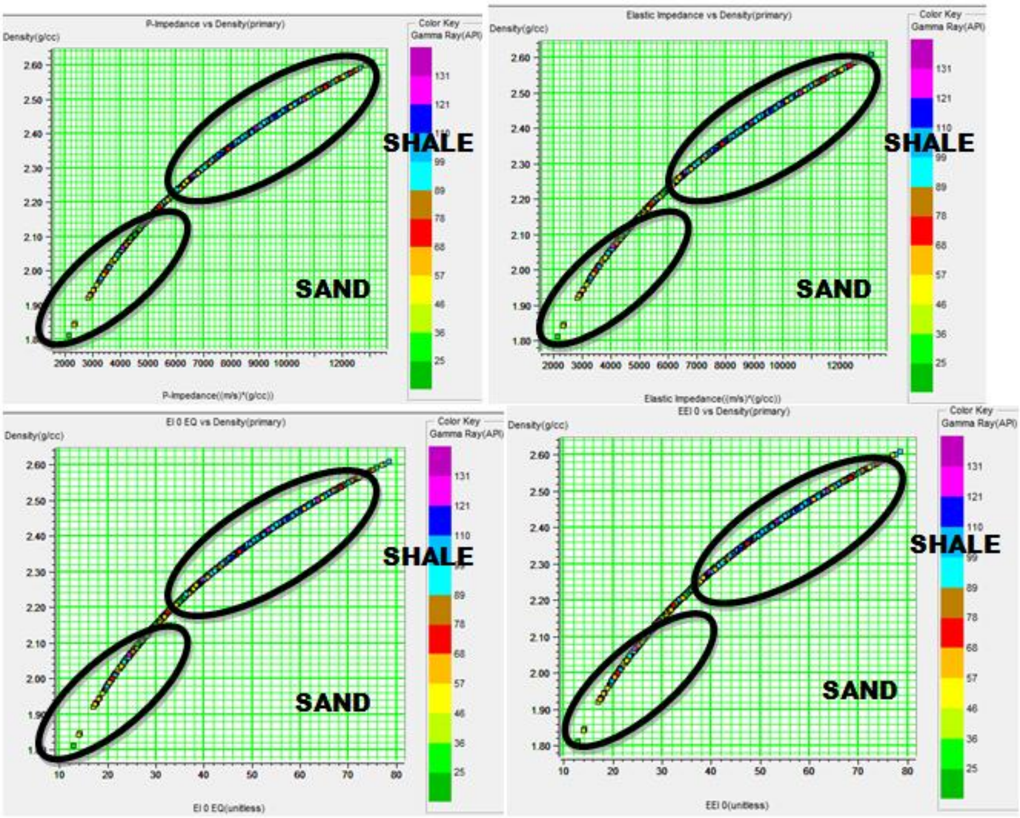

Figure 4: AI, EI(0), Derived EI (0) and Derived EEI(0) versus Density cross plot for all the target zones in Well 17 colour coded with Gamma ray.

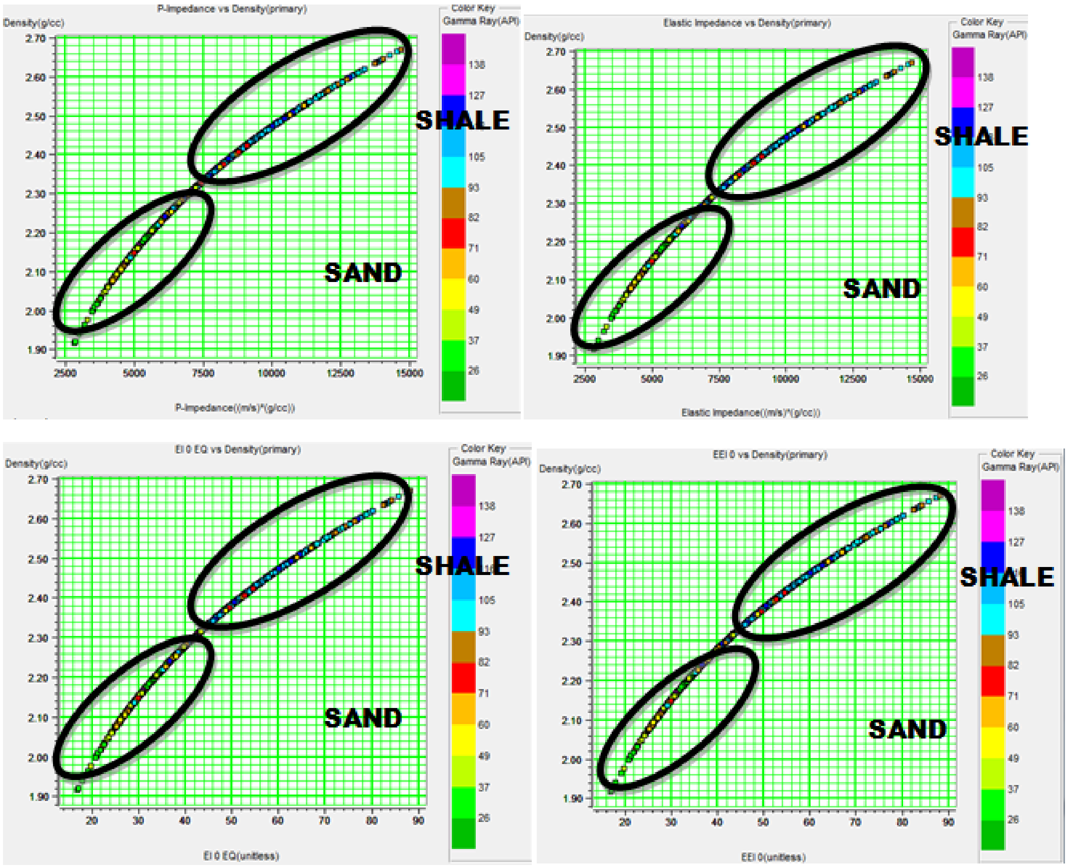

Figure 5: AI, EI(0), Derived EI (0) and Derived EEI(0) versus Density cross plot for all the target zones in Well 19 colour coded with Gamma ray.

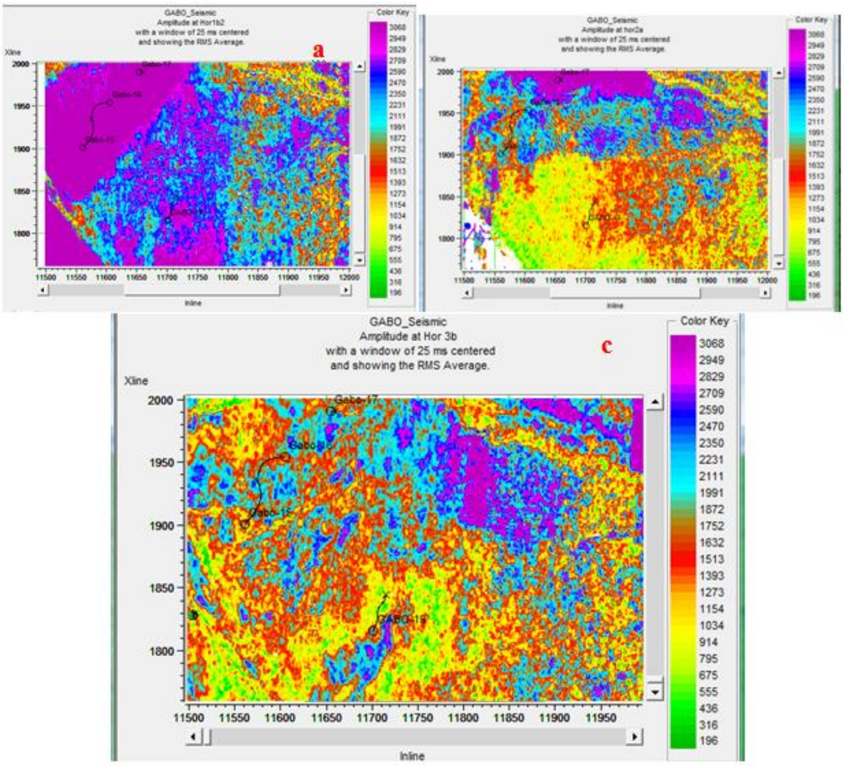

Figure 6: RMS Amplitude extraction on horizons (a) hor 1b2, (b) hor 2a and (c) hor 3b respectively from seismic volume.

The Acoustic Impedance (AI) and the Extended Elastic Impedance (EEI) generated from the modified Zoeppritz equation were inverted at zero angle. In Figure 7 (a – c), a low Acoustic Impedance (AI) values especially at well locations (Well 15, 16, and 17) which indicate hydrocarbon bearing sands at the horizons hor1b2, hor 2a and hor 3b slice respectively were observed while Well 19 lies in high Acoustic Impedance (AI) zones indicating flooding zone. Lower P-wave velocity is observed in reservoir rock containing fluids that is oil and gas which is compressible, by implication hydrocarbon bearing sands will have a lower Acoustic Impedance (AI) value than water bearing sands. From the results the Extended Elastic Impedance (EEI) inversions were robust in fluid and lithology discrimination more than the Acoustic Impedance.

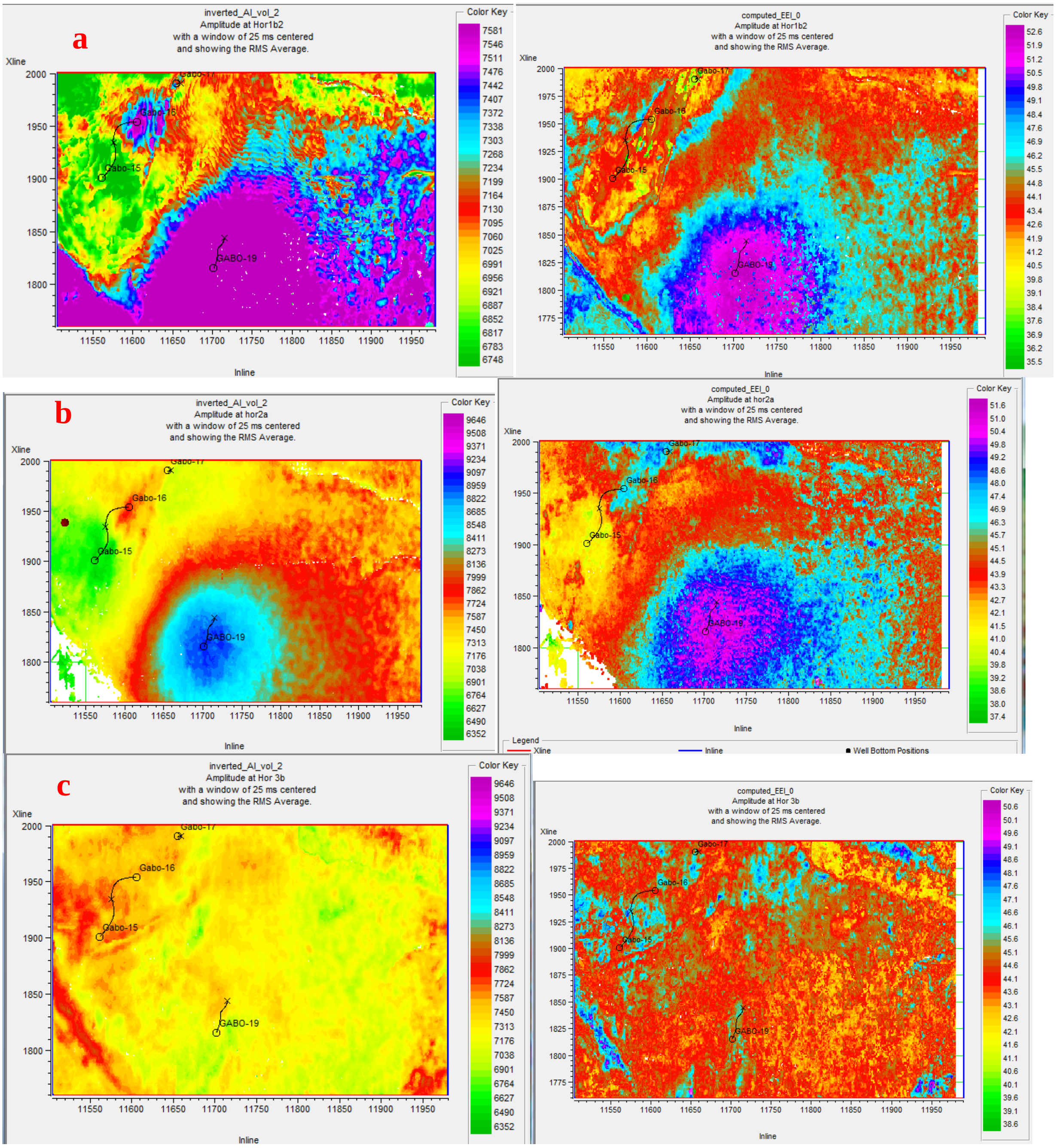

Figure 7: Comparing the data slice of inverted EEI-0 with P-impedance amplitude at hor 1b2, hor 2a and hor 3b (a – c) respectively with a window of 25ms centered.

IV. Conclusion

The modified Zoeppritz equation was used to generate Elastic Impedance (EI) and Extended Elastic Impedance (EEI) attributes which were found to be effective for lithology and fluid discrimination.

The results of the analyses show that AI, EI, derived EI and EEI at zero angle of incidences exhibit similar responses in characterizating reservoir zones and this validates our mofification to the Zoeppritz equation. The results show that the Extended Elastic Impedance (EEI) attribute effectively discriminates fluids and lithologies and thus highlights differences between reservoir and non reservoir zones. Finally, the results from the Extended Elastic impedance (EEI) inversion have shown the sensitivity and importance of conducting an Extended Elastic impedance (EEI) inversion especially in environment where Acoustic impedance (AI) alone cannot delineate hydrocarbon zones.

Acknowledgements

We acknowledge the assistance of Shell Petroleum Development Company and Total E&P Nig for graciously releasing the data to us for this work. We acknowledge CGG for their software support.

References

[1]. Latimer, R. B., Inversion and Interpretation of Impedance Data. Chapter 9 SEG, 2011; 309.
[2]. Latimer, R. B., Davidson, R and Riel, P. V., An interpreter’s guide to understanding and working with seismic-derived acoustic impedance data. The Leading Edge, 2000; 242 – 249.
[3]. Gharaee Shahri, S. A., Application of Extended Elastic Impedance (EEI) to improve Reservoir Characterization: MSc Thesis, Norwegian University of Science and Technology, Norway. 2003
[4]. Connolly, P., Elastic Impedance: The Leading Edge, 1999;438-452.
[5]. Connolly, P., Calibration and inversion of non-zero offset seismic: 68th SEG Annual Meeting, New Orleans, USA, Expanded Abstracts, 1998; 182-184
[6]. Whitcombe, D. N., Elastic impedance normalization. Geophysics, 2002; 67, 60 – 62.
[7]. Whitcombe, D., Connolly, P., Reagan, R and Redshaw, T. Extended Elastic Impedance for Fluid and Lithology Prediction, Geophysics, 2002; 67(1), 63-67.
[8]. Matthew, G., Winardhi, I. S, Application of the Extended Elastic Impedance Method and Seismic Stochastic Inversion in Mapping the Distribution of Sandstones and Gas sand in the “Lapang” Field, West Natuna Basin, Indonesia., Proceedings Indonesian Petroleum Association Thirty-Eighth Annual Convention & Exhibition, 2014
[9]. Hicks, G. J., and Francis, A. Extended Elastic impedance and its relation to AVO crossplotting and Vp/Vs. EAGE Vienna. Vienna: EAGE. 2006
[10]. Awosemo O. O., Evaluation of Elastic Impedance Attributes in Offshore High Island, Gulf of Mexico, Msc. Thesis, Department of Earth and Atmospheric Sciences, University of Houston. 2012.
[11]. Prakash, P., Singh, S. K, Chetia, B., Chaudhuri, P. K, Mohan, S., and Das, S. K. Application of Advanced Tools for Reservoir Characterization - EEI & Poisson's Impedance : A Case Study. Geohorizons. 2012; 50.
[12]. Aki, K. I. and Richards, P. G, Quantitative seismology - Theory and methods, W. H. Freeman and Company, San Francisco. 1980; I, 5.2.
[13]. Zoeppritz, K., Erdbebenwellen VIIIB, on the reflection and propagation of seismic waves: Göttinger Nachrichten, 1919; I, 66-84
[14]. Balogun, A. O. and Ebeniro, J. O, Evaluation of Seismic Attributes Generated from Extended Elastic Impedance for Lithology and Fluid Discrimination, International Journal of Science and Research (IJSR), 2017; 6(9), 776 – 779.
[15]. Balogun, A. O. and Ehirim, C. N, Lithology and Fluid Discrimination Using Bulk Modulus and Mu-Rho Attributes Generated From Extended Elastic Impedance, International Journal of Science and Research (IJSR), 2017; 6(10), 639 – 643.

Balogun A.O. and Dagogo T. "Sensitivity analysis of Extended Elastic Impedance (EEI) attributes from Modified Zoeppritz Equation."*IOSR Journal of Applied Geology and Geophysics (IOSR-JAGG),* 8(1), (2020): pp. 45-51.